

OMAERUV README File

Released: October 20, 2011

1. Overview

The NASA OMI aerosol data products consists of the aerosol extinction optical depth (AOD), aerosol absorption optical depth (AAOD), and single scattering albedo (SSA) at 354, 388 and 500 nm generated by the OMAERUV algorithm. AOD is a dimensionless measure of the extinction of light by aerosols due to the combined effect of scattering and absorption, while AAOD is that due to aerosol absorption only. The other NASA OMI aerosol product is the UV aerosol index (UVAI) produced by the OMTO3 algorithm that continues the long-term record initiated in 1978 by the TOMS sensors.

This document provides a brief description of the OMAERUV Level-2 aerosol data products derived from observations by the Ozone Monitoring Instrument (OMI) on the EOS-Aura satellite and the TOMS-like OMTO3 Aerosol Index. The information in this README file applies only to the third public release of the OMAERUV data of collection 3. As subsequent data versions are produced and released, the README file will be updated accordingly to reflect the latest algorithm modifications and data quality assessments. The OMAERUV algorithm is one of two OMI algorithms that are used to characterize the atmospheric aerosol load. A spectral fit algorithm (OMAERO) that uses measurements at several wavelengths in the range 350-500 (developed and maintained by KNMI in The Netherlands) is also applied to the OMI observations.

The OMAERUV retrieval algorithm uses a set of aerosol models to account for the presence of carbonaceous aerosols from biomass burning (BIO), desert dust (DST), and Sulfate (SLF) based aerosols (see Appendix 1). The optical depth values at 388 nm are inverted from radiance observations while the 354 and 500 nm results are obtained by conversion of the 388 nm retrievals. The conversions to 354 and 500 nm are carried out to facilitate comparisons with measurements from other space-borne and ground based sensors, as well as with model calculations, which often report values at 500 nm. However, this transformation increases the dependence on the model of aerosols assumed in the algorithm, so the reported values at the other wavelengths, particularly those at 500 nm, should be considered less reliable.

The file also contains the geo-location information associated with each OMI pixel in the global observation mode, as well as ancillary information used in the inversion procedure. In the global mode each file contains a single orbit of data covering the sunlit portion of the Earth from pole-to-pole with a swath width of approximately 2600 km.

Because of the large sensitivity of the OMI near UV observations to particle absorption, the AAOD is the most reliable quantitative OMAERUV aerosol parameter. Since, by definition, AAOD is insensitive to clouds, the AAOD retrieval can be extended to pixels with small amounts for cloud contamination and is not restricted to completely cloud-free scenes as it is the case for the AOD retrieval.

For environments where cloud free conditions prevail, the AOD can be reliably retrieved. Cloud interference with the satellite retrieval is minimal over arid and semi-arid regions where dust aerosols are commonly present. Clear skies are also frequent in areas of seasonal biomass burning and forest fires in the vicinity of the sources. As the plumes of dust and smoke aerosols drift away from their source regions, they mix with clouds and the OMAERUV AOD retrieval becomes very challenging.

Please refer to the OMAERUV and OMTO3 release specific information files for details on software versions and known problems.

The UVAI is a measure of the departure of the spectral dependence of the near-UV upwelling radiation at the top of the actual Earth surface-atmosphere system from that of a hypothetical pure molecular atmosphere bounded at the bottom by a wavelength independent Lambertian surface. The UVAI concept was developed empirically from TOMS observations. Near-zero values of UVAI result when the radiative transfer processes accounted for in the simple Rayleigh scattering model adequately explain the observations. For a well-calibrated sensor, the non-zero residues are produced solely by geophysical effects, of which absorbing aerosols are by far the most important source of positive UVAI values. Non-absorbing aerosols yield small negative UVAI values but the difficulty to separate the non-absorbing aerosol signal from other non-aerosol related effects limits its usefulness.

The UVAI has become an invaluable tool for tracking long-range transport of absorbing aerosols (smoke and dust) throughout the globe, even when the aerosols are over clouds. The UVAI has been instrumental in the discovery of important aspects of aerosol transport both horizontally and vertically. For instance, UVAI observations indicate that smoke aerosol plumes generated by boreal forest fires at mid and high latitudes are associated with the formation of pyro-cumulonimbus clouds capable of transporting carbonaceous aerosols to the lower stratosphere. Although these aerosols intrusions had been detected by SAGE and POAM observations, their connection to biomass burning was unequivocally established by UVAI observations [Fromm et al, 2005].

The UVAI is very nearly proportional to AAOD over both dark scenes as well as over clouds and snow/ice. However, since the proportionality constant varies with aerosol type, height, and the scene brightness, it is not yet possible to

convert the information content of the UVAI into AAOD, except over dark cloud-free scenes. The mathematical definition of UVAI is given in section 3.

2. Algorithm Upgrades in Version V1.3.7 (this release)

A brief listing of the algorithm upgrades implemented in the current release is presented here. A more detailed description of the upgrades is presented in the Algorithm Description section below. For a history of algorithm upgrades see appendix 2.

2.1 New set of carbonaceous aerosol models

The carbonaceous (BIO) aerosol model has been replaced with a new model that includes wavelength-dependent imaginary component of the refractive index (see Appendix 1). This change allows for the presence of organic carbon (OC) as a light-absorbing aerosol component [Jethva and Torres, 2011]. The previous aerosol model implicitly assumed black carbon (BC) as the only absorbing component.

2.2 Aerosol Type Identification

The differentiation between carbonaceous and desert dust aerosols has been improved by making use of column carbon monoxide (CO) measured by the AIRS sensor on the Aqua satellite. CO is the most abundant gaseous component of carbonaceous aerosols and is, therefore, a reliable tracer of biomass burning aerosols. The aerosol type selection is based on the combined use of the OMI UV Aerosol Index (UVAI) and the CO amount. The short time difference of only few minutes between Aura-OMI and Aqua-AIRS observations allows the use of the two observations to characterize almost the same scene. See section 3 for a detailed description of the procedure to identify the aerosol type.

2.3 New Climatology of aerosol layer height based on CALIOP data

When either the BIO or DST aerosol type has been selected the aerosol layer height is primarily determined by a monthly global climatology derived from CALIOP observations. When the aerosol layer height is not available from CALIOP climatology (generally at high latitudes in both hemispheres) the height is obtained as in the previous version of the algorithm based on the climatology from GOCART model inferred aerosol heights. See section 3 for details.

2.4 Changes in look-up table configuration

- The number of solar zenith angle nodal points in the look-up tables has increased from 5 [0, 20, 40, 60, 80] to 7 [0, 20, 40, 60, **66**, **72**, 80] for all aerosol models.

- The number of AOD nodal points has changed from 6 [0.0, 0.1, 0.5, 1.0, 2.5, 4.0] to 7 [0.0, 0.1, 0.5, 1.0, 2.5, 4.0, **6.0**] for all aerosol models.

2.5 Other changes

- The low limit AI threshold for aerosol retrievals has been lowered to 0.8 over the oceans.

-A field containing the reporting wavelengths [354, 388, 500 nm] has been added to the level2 file and removed from the swath attributes field.

-Information of aerosol layer heights (0.0, 1.5, 3.0, 6.0, 10.0 km) is available in the swath attributes field.

- Row anomaly exclusion rules have been updated

The updated information of row anomaly from the XtrackQualityFlags field in OMI L1b swath file is used for screening row anomaly affected scenes before retrieving aerosol products.

The XtrackQualityFlags field has been added to the Geolocation Fields of level 2 file. The information of bit values for this field is available at the site (<http://www.knmi.nl/omi/research/product/rowanomaly-background.php>).

Row anomaly screened scenes are also reported as the value of 8 in the AlgorithmFlags field. It is possible to find additional row anomalies not fully characterized in the data so that care must be taken in using data since 2009. A further improved flagging scheme is under development and will be updated periodically as new anomaly develops.

3. Algorithm Description

Though OMI is a hyper-spectral instrument and measures over a wide wavelength range from UV to blue (270-500nm), the OMAERUV aerosol algorithm currently uses the measurements made at just two wavelengths: 354 and 388 nm. This is partly to maintain heritage with similar algorithm used for TOMS [Torres et al, 1998], and partly because of lack of reliable surface reflectance data at the longer OMI wavelengths. Wavelengths below 330 nm cannot be used due to strong ozone absorption.

3.1 Aerosol Optical Depth and Single Scattering Albedo

There are two advantages of the near-UV technique for deriving aerosol properties. In the UV, the reflectance of all terrestrial surfaces is very low,

therefore, the retrieval of aerosol properties is possible over both water and land surfaces, including the arid and semi-arid regions of the world that appear very bright in the visible and near-IR. The second advantage is that interaction between aerosol absorption and molecular scattering from below the aerosol layer allows one to estimate AAOD.

The OMAERUV retrieval algorithm assumes that the column atmospheric aerosol load can be represented by one of three types of aerosols: desert dust (DST), carbonaceous aerosols associated with biomass burning (BIO), and weakly absorbing sulfate-based aerosols (SLF). Each aerosol type is represented by seven aerosol models of varying single scattering albedo, for a total of twenty-one models. The micro-physical properties of the twenty-one aerosol models used by OMAERUV are based on long-term statistics of ground-based observations by the Aerosol Robotic Network (AERONET). For a full description of the aerosol models see Appendix 1. Given an aerosol type we calculate 354 and 388 nm reflectances in the OMI measurement geometry for a range of values of optical thickness and single scattering albedo using Mie scattering radiative transfer calculations. An absorbing aerosol index using observations at 354 and 388 nm ($UVAI_0$) is calculated in OMAERUV for internal use in the AOD and SSA retrieval scheme. Unlike the OMT03 UVAI, that is based in the combined use of the LER and MLER approximations, the OMAERUV $UVAI_0$ only uses the LER model.

The current characterization of ocean reflective properties in the OMAERUV algorithm does not explicitly account for ocean color effects and, therefore, the quality of the retrieved aerosol properties over the oceans for low aerosol amounts would be highly uncertain. For that reason, retrievals over the oceans are only carried out for high concentrations of either desert dust or carbonaceous aerosols as indicated by $UVAI_0$ values larger than or equal to 0.8. Over the oceans $UVAI_0$ values less than 0.8 are associated with ocean color effects and/or low concentration weakly absorbing (or non-absorbing) aerosols.

3.1.1 Surface Albedo

A climatological data-set of surface albedo derived from TOMS observations at 331, 340, 360 and 380 nm is used to characterize surface reflective properties. Surfaces are assumed to be Lambertian. This data set replaces the climatology of Herman and Celarier [1997] that did not account for the spectral dependence of UV surface albedo. Surface albedo values at 354 and 388 nm are obtained by interpolation of the TOMS-based climatology (354 nm values are interpolated between 340 and 360 nm values but 380 nm surface albedo is used instead of extrapolation to 388 nm).

3.1.2 Aerosol type selection

The selection of an aerosol type makes use of the $UVAI_0$ and the total column carbon monoxide (CO) given in molecules-cm⁻², derived from AIRS

observations. Since CO is the main gaseous component of biomass burning it constitutes a reliable tracer of carbonaceous aerosol. As used in OMAERUV, the CO is reduced to a unitless quantity by dividing it by 10^{18} molecules-cm⁻². Figure 1 illustrates the combined use of CO and $UVAI_o$ measurements to select the predominant aerosol type.

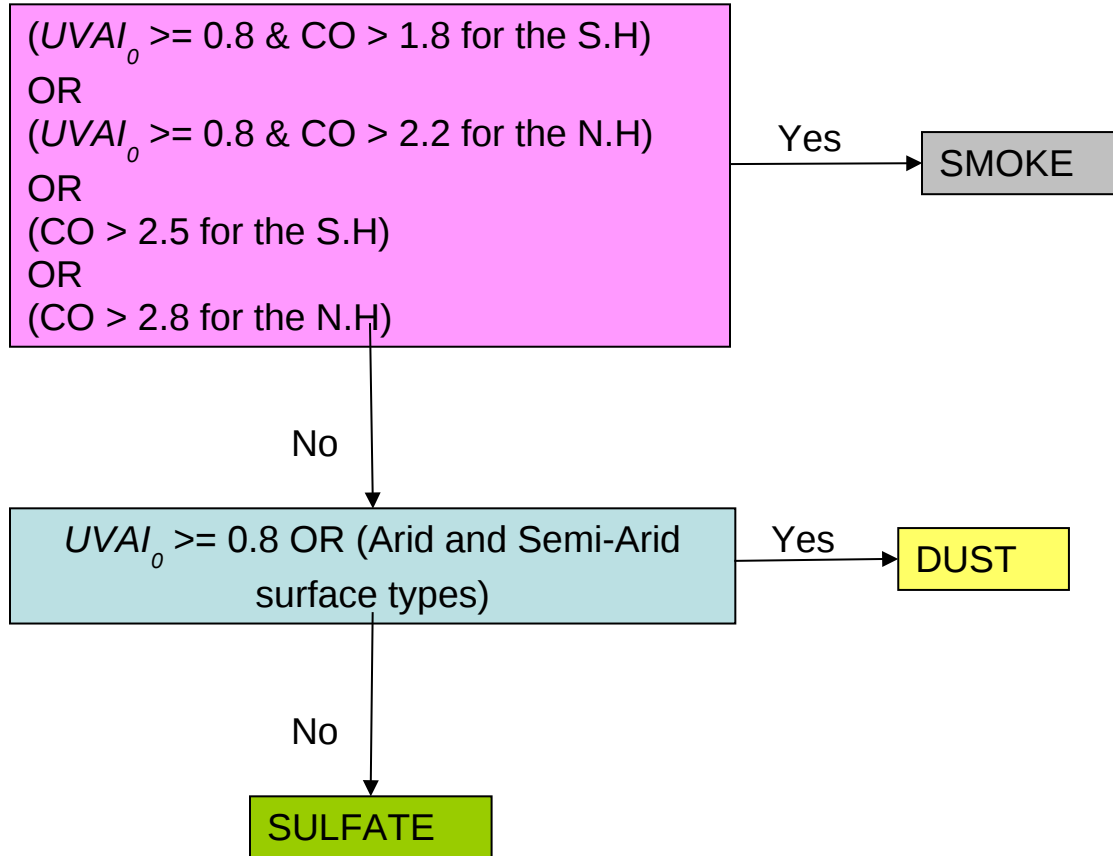


Figure 1. Flow diagram illustrating the use of UVAI and CO parameters for aerosol type selection.

Different CO threshold values are used for the northern and southern hemispheres to remove upper tropospheric CO which may not be necessarily associated with carbonaceous aerosols.

3.1.3 Aerosol layer height

The height above the surface of absorbing aerosol layers (desert dust and smoke particles) is given by a climatological data set derived from CALIPSO observations. The climatology covers most regions of the globe where seasonally varying loads of desert dust and carbonaceous are known to reside.

The choice of aerosol layer height for absorbing aerosol layers over areas not covered by the provided climatology varies with aerosol type and location. Carbonaceous aerosol layers between within 30 degrees of the Equator are assumed to have maximum concentration at 3 km above ground level, whereas mid and high-latitude (pole wards of $\pm 45^\circ$) smoke layers are assumed to peak at 6 km. The height of smoke layers between 30° and 45° latitude in both hemispheres is interpolated with latitude between 3 and 6 km. The location of desert dust aerosol layers varies between 1.5 and 10 km, and is given by a multi-year climatological average of Chemical Model Transport (CTM) calculations using the GOCART model.

For the sulfate-based aerosols, the algorithm considers that the aerosol concentration is largest at the surface and decreases exponentially with height.

3.1.4 Retrieval Products

Retrieved values of AOD, AAOD and SSA are reported at 388 nm. Similar values are also reported at 354 and 500 nm by conversion from the 388 nm retrieval. The wavelength conversion from 388 nm to 354 and 500 nm is done using the spectral dependence associated with the assumed aerosol particle size distribution and retrieved absorption information.

3.1.5 Algorithm Flag

A simplified algorithm flag scheme has been implemented. Flag categories and their description are summarized in Table 1.

More detailed description of the algorithm is available in the Algorithm Theoretical Basis Document (ATBD) on http://eospsso.gsfc.nasa.gov/eos_homepage/for_scientists/atbd/docs/OMI/ATBD-OMI-03.pdf

3.2 UV Aerosol Index (UVAI)

A TOMS-like UVAI is calculated from OMI measurements at 331 and 360 nm. The UVAI is basically a residual quantity resulting from the comparison between measured and calculated radiances (L_{λ}^{obs} and L_{λ}^{cal} respectively) in the range 330-390 nm where gas absorption effects are negligible. The calculated radiance is obtained using a simple model of the earth-atmosphere system consisting of a molecular atmosphere bounded at the bottom by a Lambert Equivalent Reflector (LER) [Dave and Mateer, 1967]. A key assumption in this model representation of the earth-atmosphere system is that the reflectivity R of the column atmosphere's lower boundary is wavelength independent in the near

UV. In the above described model, the upwelling near UV radiance at the top of the atmosphere is given by the expression

$$L_{\lambda}(\theta, \theta_0, \varphi, p_0) = L_{\lambda}^0(\theta, \theta_0, \varphi, p_0) + \frac{R_{\lambda} T_{\lambda}(\theta, \theta_0, p_0)}{1 - R_{\lambda} S_{\lambda}^b(p_0)} \quad (1)$$

where L_{λ}^0 is the radiance scattered by the atmosphere or path radiance, T_{λ} represents the total amount of direct plus diffuse radiation reaching the surface, multiplied by the atmospheric transmission of the diffuse component in the direction of the sensor. The numerator in the second term of equation 1 accounts for the once-reflected radiation whereas multiple reflections by the surface is accounted for in the denominator where S_{λ}^b is the spherical albedo that accounts for the fraction of the reflected radiation scattered back to the surface by the atmosphere.

In the OMTO3 algorithm the upwelling radiation at the top of the atmosphere is assumed to result from the combined effect of radiances originating a two pressure levels in the atmosphere representing surface, L_{λ}^s , and clouds, L_{λ}^c . Both terms are calculated for a Rayleigh atmosphere. The L_{λ}^s term is calculated for the pressure level associated with the average ground terrain height and a surface albedo, R_s , of 0.15. The L_{λ}^c component on the other hand, is calculated for the cloud pressure corresponding to the cloud height which can be independently measured or assumed making use of available cloud height climatological data. In the OMTO3 algorithm the cloud pressure is taken from the OMCLDRR product [Joiner and Vassilkov, 2006]. The albedo of the elevated surface representing the cloud, R_c , is assumed to be 0.80.

The way L_{λ}^{cal} is calculated depends on the magnitude of the observed quantity $L_{\lambda_0}^{obs}$ at wavelength λ_0 in relation to the theoretically determined values of $L_{\lambda_0}^s$ and $L_{\lambda_0}^c$.

If $L_{\lambda_0}^{obs} < L_{\lambda_0}^s$ or $L_{\lambda_0}^{obs} < L_{\lambda_0}^c$ R_{λ_0} is calculated using the LER approximation by simply solving for R in equation 1 yielding

$$R_{\lambda_0} = \frac{L_{\lambda_0}^{obs} - L_{\lambda_0}^0}{T_{\lambda_0} + S_{\lambda_0}^b (L_{\lambda_0}^* - L_{\lambda_0}^0)} \quad (2)$$

where the dependence variables have been dropped for simplicity. The resulting reflectivity is then used back in equation (1) to find L_{λ}^{cal} at a wavelength other than λ_0 ,

$$L_{\lambda}^{cal} = L_{\lambda}^0 + \frac{R_{\lambda_0} T_{\lambda}(\theta, \theta_0, p_0)}{1 - R_{\lambda_0} S_{\lambda}^b(p_0)} \quad (3)$$

The aerosol Index is then calculated using equation (6) below.

If $L_{\lambda_0}^s \leq L_{\lambda_0}^{obs} \leq L_{\lambda_0}^c$, then an effective cloud fraction f is derived using

$$f = \frac{L_{\lambda_0}^{obs} - L_{\lambda_0}^s}{L_{\lambda_0}^c - L_{\lambda_0}^s} \quad (4).$$

The parameter f , is then used to calculate L_{λ}^{cal} as a linear combination of L_{λ}^s and L_{λ}^c ,

$$L_{\lambda}^{cal} = (1 - f)L_{\lambda}^s + fL_{\lambda}^c \quad (5)$$

In the OMT03 algorithm λ_0 (reference wavelength) is 331 nm and λ is 360 nm.

The approach represented by equation (5), in which clouds are modeled as elevated highly reflective Lambertian surfaces is generally referred to as the Mixed LER (or MLER) model as opposed to the simpler LER approach of equation (3) used to represent cloud-free conditions. Although the LER model works very well under cloud-free conditions, *Ahmad et al.* [2004] showed that the MLER approximation does a better job in explaining actual observations in the presence of clouds and works equally well to Mie scattering calculations using the Parallel Cloud (PC) approximation.

The residue, r_{λ} is defined as the natural log of the ratio of the actually measured radiance L_{λ}^* to the calculated value L_{λ}^{cal} ,

$$r_{\lambda} = -100 \log \left[\frac{L_{\lambda}^*}{L_{\lambda}^{cal}} \right] \quad (6).$$

This residual quantity provides a measure of the error in predicting the actually observed spectral contrast using the LER/MLER approximation [*Torres et al.*, 1998].

By definition, when $\lambda_0 > \lambda$ $UVAI = r_{\lambda}$. In the OMT03 algorithm where $\lambda_0 < \lambda$, $UVAI = -r_{\lambda}$

4. Data Quality Assessment

Because of the relatively large footprint of the OMI observations (13x24 km² at nadir), the major factor affecting the quality of aerosol products is sub-pixel cloud contamination. Currently the cloud mask is based on simple reflectivity and $UVAI_0$ thresholds, which can cause significant overestimation of the mean AOD. However, experience with TOMS suggests that monthly mean AODs do reliably capture variation in the AOD with time. It is important to note, however, that the AAOD is less affected by cloud contamination and hence is more reliable.

In general OMAERUV retrievals are more reliable over land than over water surfaces. The near-UV retrieval method is particularly sensitive to carbonaceous and mineral aerosols. The sources of these aerosol types are located over the continents, and the atmospheric aerosol load associated with these events is generally large. In addition, dust and smoke aerosol events tend to take place under meteorological conditions which do not favor the formation of

clouds in the vicinity of the sources, such as arid and semi-arid areas in the case of dust, and the dry season in the case of biomass burning. The OMAERUV retrieved AOD of sulfate-based aerosols is less accurate due to its low values, higher spatial variability and increased levels of sub-pixel cloud contamination.

Ocean OMAERUV retrievals are affected by other factors. In addition to sub-pixel clouds, the ocean surface reflectance show distinct angular and spectral variations (compared to land) due to spectrally varying scattering from the water, often called water-leaving radiances. (WLR), chlorophyll, sediments and other types of suspended matter decrease WLR. Spectral variations of ocean reflectance are accounted for in a climatological sense using a wavelength dependent surface reflectance data set. Short-term variability, however, is not taken into account in the current version of the algorithm. Ocean retrievals of AOD and AAOD are not reported for sun glint angles smaller than 40° or for scenes where $UVAI_0$ is less than 0.8.

Integer Value	Algorithm Flag Description

Aerosol extinction optical depth (AOD), Single Scattering Albedo(SSA), and Aerosol Absorption Optical Depth(AAOD) Retrievals	
0	Most reliable (AAOD, SSA, and AOD)
1	Reliable (AAOD only), AOD and SSA non- reliable.
2	Non reliable (AAOD, SSA, and AOD) , qualitative use only
Not Reliable/no retrievals	
3	Out-of-bounds SSA or AOD above 6.0 at 500nm.
4	Cloud/snow/ice contaminated data.
5	Solar Zenith Angle above threshold (70 degree).
6	Sun glint angle below threshold over water (40 degree).
7	Terrain Pressure below threshold (628.7hPa).
8	Cross track anomaly.

Table 1. Algorithm flag scheme
(consistent with the file specification document OMAERUV.fs)

The AOD over land is expected to have the same root –mean square (rms) error as TOMS retrievals (0.1 or 30% whichever is larger). The rms error in AOD over water is likely to be 2 times larger. The rms error for AAOD is estimated to be ~0.01.

Comparisons of OMAERUV retrieved optical depth to AERONET observations at several sites are shown in Figure 2. The sample comparison includes sites where the atmospheric aerosol load typically consists of urban aerosols (Baltimore, Maryland Science Center site); carbonaceous aerosols (Brazil, Alta Floresta, site); desert dust (Saharan Desert, Tamanrasset site); and industrial pollution aerosols (Eastern China, XiangHe site). In general when cloud-free conditions prevail OMAERUV-observed AOD values are in reasonable agreement with AERONET. The level of agreement is very good with correlation coefficients between 0.79 and 0.92, slopes in the range 0.63-0.92; and intercepts between 0.08 and 0.18.

For environments where sub-pixel cloud contamination is persistent during all seasons the statistics of the OMAERUV-AERONET comparisons are poor. For these conditions comparisons over a longer period are needed to better assess the quality of the OMI aerosol product.

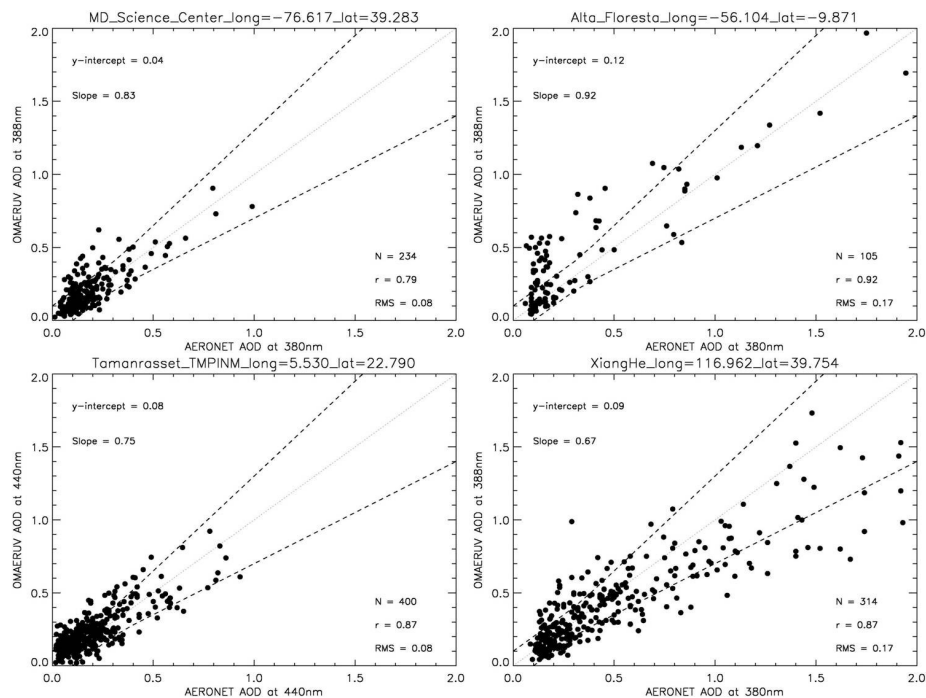


Figure 2. OMAERUV-AERONET comparison of aerosol optical depth. For the comparison at Tamanrasset, the OMI retrieval has been converted to 440 nm.

As part of the data quality assessment OMAERUV retrievals of AOD have been compared to MODIS data for different aerosol types. In general, when clear conditions predominate, the OMAERUV and MODIS AOD products are well correlated, especially for large-scale dust and smoke events. For background aerosol conditions, sub-pixel cloud contamination significantly affects the OMI retrieval.

The OMAERUV retrieved 388 nm single scattering albedo has been evaluated by comparison to AERONET retrievals at several sites. Figure 3 shows examples of such comparisons at the Banizoumbou and Dakar sites in northern Africa. The OMI result has been converted to 440 nm for this analysis. At the Banizoumbou site 50% of the retrievals agree with AERONET's within 0.03 (dashed line) whereas 77% agree within 0.05. In Dakar the level of agreement is 63% and 86% respectively.

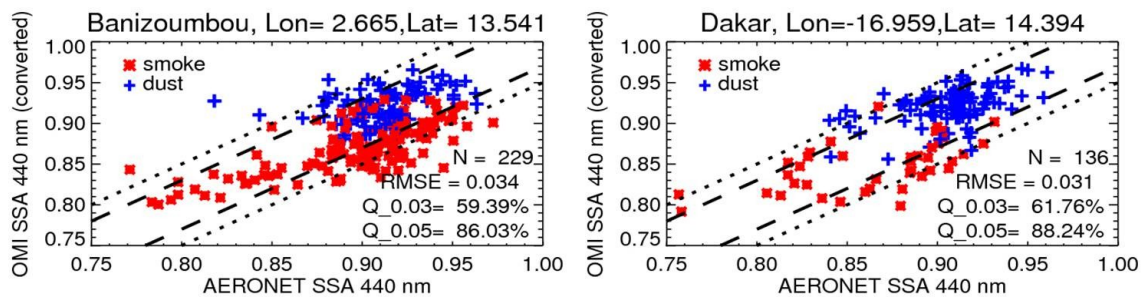


Figure 3. OMAERUV-AERONET comparison of single scattering albedo.

5. Product Description

A 2600-km wide OMI swath contains 60 pixels. Due to optical aberrations and a small asymmetry between the instrument optic axis with the S/C nadir, the pixels on the swath are not symmetrically aligned on the line perpendicular to the orbital plane. However, the latitude and longitude provided with each pixel represent the location of each pixel on the ground to a fraction of a pixel.

The OMAERUV product is written as an HDF-EOS5 swath file. For tools to read HDF-EOS5 data files, please visit the link: <http://disc.gsfc.nasa.gov/Aura/tools.shtml>.

A single OMAERUV file contains information retrieved from each OMI pixel over the sun-lit portion of one Aura orbit. The data are ordered in time.

These files includes latitude, longitude, viewing geometry, best estimate values of AOD (variable name FinalAerosolOpticalDepth) and AAOD (variable name FinalAerosolAbsOpticalDepth) at 352, 388 and 500 nm associated with a reported particular choice of aerosol vertical distribution, and ancillary parameters used in the retrieval scheme.

A very important parameter also reported is the algorithm quality flag (field name AlgorithmFlags), which contains the processing error flag in its first byte. Most users should use data with a data quality flag 0 and 1. For a complete list of the parameters, please read the [OMAERUV file specification](#). Gridded products will also be available. Please check the [Goddard Earth Sciences \(GES\) Data and](#)

[Information Services Center \(DISC\) website](#) for current information on these products.

Full OMAERUV and OMT03 aerosol data, as well as subsets of these data over many ground stations and along Aura validation aircraft flights paths are also available through the [Aura Validation Data Center \(AVDC\) website](#) to those investigators who are associated with the various Aura science teams.

Questions related to the OMAERUV and OMT03 aerosol dataset should be directed to the [GES DISC](#). For questions and comments related to the OMAERUV and OMT03 aerosol algorithms and data quality, please contact Omar Torres (omar.o.torres@nasa.gov) who has the overall responsibility for these products.

References and related publications

Ahmad, Z., P. K. Bhartia, and N. Krotkov (2004), Spectral properties of backscattered UV radiation in cloudy atmospheres, *J. Geophys. Res.*, 109, D01201, doi:10.1029/2003JD003395.

Ahn C., O. Torres, and P.K. Bhartia (2008), Comparison of OMI UV Aerosol Products with Aqua-MODIS and MISR observations in 2006, *J. Geophys. Res.*, 113, D16S27, doi:10.1029/2007JD008832.

Dave, J.V., and C.L. Mateer (1967), A preliminary study on the possibility of estimating total atmospheric ozone from satellite measurements, *J. Atm Sci.*, 24, 414-427

Fromm, M., R. Bevilacqua, R. Servranckx, J. Rosen, J.P. Thayer, J. Herman, and D. Larko, Pyro-cumulonimbus injection of smoke to the stratosphere: Observations and impact of a super blowup in northwestern Canada on 3-4 August 1998, *J. Geophys. Res.*, 110, doi:10.1029/2004JD005350, 2005

Herman, J.R., and E. A. Celarier, Earth surface reflectivity climatology at 340 and 380 nm from TOMS data, *J. Geophys. Res.*, 102, 28,003-28,011, 1997

IGBP, http://www-surf.larc.nasa.gov/surf/pages/sce_type.html

Jethva, H. and O. Torres (2011): Satellite-based evidence of wavelength-dependent aerosol absorption in biomass burning smoke inferred from ozone monitoring instrument, *Atmos. Chem. Phys.*, 11, 10541-10551, doi:10.5194/acpd-11-7291-2011.

Joiner J. and A.P. Vasilkov, First Results From the OMI Rotational Raman Scattering Cloud Pressure Algorithm, IEEE Trans. Geo. Rem. Sens., 2006, Vol. **44**, No. 5, 1272-1282, [doi:10.1109/TGRS.2005.861385](https://doi.org/10.1109/TGRS.2005.861385).

Livingston, J.M., J. Redemann, P. B. Russell, O. Torres, B. Veihelmann, P. Veefkind, R. Braak, A. Smirnov, L. Remer, R. W. Bergstrom, O. Coddington, K. S. Schmidt, P. Pilewskie, R. Johnson, and Q. Zhang (2009), Comparison of aerosol optical depths from the Ozone Monitoring Instrument (OMI) on Aura with results from airborne sunphotometry, other space and ground measurements, Atmos. Chem. Phys. Discuss., 9, 6743-6765

Torres, O., A. Tanskanen, B. Veihelman, C. Ahn, R. Braak, P. K. Bhartia, P. Veefkind, and P. Levelt (2007), Aerosols and Surface UV Products from OMI Observations: An Overview, , *J. Geophys. Res.*, 112, D24S47, doi:10.1029/2007JD008809.

Torres O., P.K. Bhartia, J.R. Herman and Z. Ahmad, Derivation of aerosol properties from satellite measurements of backscattered ultraviolet radiation. Theoretical Basis, *J. Geophys. Res.*, 103, 17099-17110, 1998

Torres, O., P.K. Bhartia, A. Syniuk, and E. Welton, TOMS Measurements of Aerosol Absorption from Space: Comparison to SAFARI 2000 Ground based Observations, *J. Geophys. Res.*, 110, D10S18, doi:10.1029/2004JD004611, 2005

APPENDIX 1

OMI BIO AEROSOL MODELS

Real refractive index 1.50 (wavelength independent)

Models 1:3

R_F	R_C	σ_F	σ_C	Fraction
0.087	0.567	1.537	2.203	$2.06 \cdot 10^{-4}$

Nodal points on imaginary refractive index (wavelength dependent):

354.0 nm: 0.00000, 0.0060, 0.0120, 0.0240, 0.0360, 0.0480, 0.0576

388.0 nm: 0.00000, 0.0050, 0.0100, 0.0200, 0.0300, 0.0400, 0.0480

Models 4:7

R_F	R_C	σ_F	σ_C	Fraction
0.08	0.705	1.492	2.075	$2.05 \cdot 10^{-4}$

Nodal points on imaginary refractive index (wavelength dependent):

354.0 nm: 0.00000, 0.0060, 0.0120, 0.0240, 0.0360, 0.0480, 0.0576

388.0 nm: 0.00000, 0.0050, 0.0100, 0.0200, 0.0300, 0.0400, 0.0480

OMI DST AEROSOL MODELS

Real refractive index 1.55 (wavelength independent)

Models 1:7

R_F	R_C	σ_F	σ_C	Fraction
0.052	0.67	1.697	1.806	$4.35 \cdot 10^{-3}$

Nodal points on imaginary refractive index (wavelength dependent):

354.0 nm: 0.00000, 0.00128, 0.00256, 0.00561, 0.00832, 0.01279, 0.02303

388.0 nm: 0.00000, 0.00092, 0.00185, 0.00405, 0.00600, 0.00923, 0.01662

OMI SLF AEROSOL MODELS

Models 1:7

Real refractive index 1.40 (wavelength independent)

R_F	R_C	σ_F	σ_C	Fraction
0.088	0.509	1.499	2.160	$4.04 \cdot 10^{-4}$

Nodal points on imaginary refractive index:

0.000, 0.002, 0.004, 0.006, 0.008, 0.010, 0.012 (wavelength independent)

R_F & R_C are Radii for Fine and Coarse Mode Aerosols
 σ_F & σ_C are the Standard Deviations

APPENDIX 2

History of Algorithm Upgrades

1. Algorithm Version V1.1.1 (October 31, 2007)

The use of a new calibrated OMI level1b (L1b) radiance data set is most important change in this release. The collection 003 L1b data includes a radiometric correction as well as an adjustment for stray light effects. The first correction is largely spectrally independent whereas the latter is wavelength dependent. The OMI L1b products are available through the NASA S4PA system (<http://disc.gsfc.nasa.gov/Aura/OMI/index.shtml>).

Threshold values of reflectivity and UV aerosol index used for aerosol type selection and assignment of algorithm flags were modified as shown in Table 1.

Sun glint angle threshold over the oceans for Aerosol Index calculation has been lowered from 40° to 20°.

2. Algorithm Version V1.1.6 (March 31, 2009)

A major algorithm modification was implemented earlier in this version. Aerosol retrievals over the oceans are carried out only if the UVAI is larger than one. When $UVAI \leq 1.0$ no retrieval is performed and fill values are reported.

Over the oceans UVAI values less than one are associated with ocean color and/or low aerosol concentration weakly absorbing (or non-absorbing) aerosols. Since the current representation of ocean surface effects in the OMAERUV algorithm does not explicitly correct for ocean color signal, the quality of the retrieved aerosol properties over the oceans for low aerosol amounts is highly uncertain.

Other algorithm changes:

- Changes to aerosol retrieval over land for $UVAI \leq 1.0$ (See algorithm description)
- Reported Retrieved Products: Aerosol Extinction Optical Depth, Aerosol Absorption Optical Depth and Single Scattering Albedo at 354, 388 and 500 nm.
- Changes in prescribed aerosol layer height when aerosol type is identified as carbonaceous (BIO). See Algorithm Description section below.

- Row anomaly Exclusions:

Several row anomalies have occurred in the recent past. These anomalies affect the quality of the OMAERUV data products. In this version of the Algorithm the following rows are excluded, i.e., no retrieval are reported

- Row Anomaly Exclusion Rules

1. (54 and 55; 1-based) since June 1, 2007.
2. (38 – 43) since May 1, 2008.
3. (36 – 45) since Dec 1, 2008
4. (29 – 45) since Jan 24, 2009.